

Central Lancashire Online Knowledge (CLoK)

Title	Performance investigation of a micro-channel flat separated loop heat pipe system for data centre cooling
Туре	Article
URL	https://clok.uclan.ac.uk/id/eprint/38795/
DOI	https://doi.org/10.1093/ijlct/ctaa036
Date	2020
Citation	Hu, Menglong, Luo, Liang, Badiei, Ali, Chen, Fucheng, Zheng, Siming, Wang, Zhangyuan and Zhao, Xudong (2020) Performance investigation of a microchannel flat separated loop heat pipe system for data centre cooling. International Journal of Low-Carbon Technologies, 16 (1). pp. 98-113. ISSN 1748-1317
Creators	Hu, Menglong, Luo, Liang, Badiei, Ali, Chen, Fucheng, Zheng, Siming, Wang, Zhangyuan and Zhao, Xudong

It is advisable to refer to the publisher's version if you intend to cite from the work. https://doi.org/10.1093/ijlct/ctaa036

For information about Research at UCLan please go to http://www.uclan.ac.uk/research/

All outputs in CLoK are protected by Intellectual Property Rights law, including Copyright law. Copyright, IPR and Moral Rights for the works on this site are retained by the individual authors and/or other copyright owners. Terms and conditions for use of this material are defined in the http://clok.uclan.ac.uk/policies/

Performance investigation of a micro-channel flat separated loop heat pipe system for data centre cooling

Menglong Hu¹, Liang Luo¹, Ali Badiei², Fucheng Chen¹, Siming Zheng¹, Zhangyuan Wang^{1,2,*} and Xudong Zhao²

¹School of Civil and Transportation Engineering, Guangdong University of Technology, 100 Waihuan Xi Road, Higher Education Mega Centre, Guangzhou 510006, Guangdong Province, P.R. China ²Centre for Sustainable Energy Technologies, University Hull, Cottingham Road, Hull, HU6 7RX, UK

Abstract

This paper investigates a novel micro-channel flat separated loop heat pipe system for cooling the information technology equipment in the data centres through theoretical and experimental analysis and by assessing the impact of the inlet water temperature on system performance. A computer model is developed to simulate the steady-state performance of the micro-channel flat separated loop heat pipe system. After comparing the experimental and modelling results, the new and conventional system under the same working conditions, the model is validated yielding high accuracy in predicting the performance of the micro-channel flat separated loop heat pipe system with recorded error being limited to 2.16–8.97%. The new system has better performance than the conventional system. Under the operating conditions of heat load intensity of 1,000 W/m², water flow rate of 0.28 m³/h, refrigerant filling rate of 30%, ambient air temperature of 26°C, and evaporator and condenser height difference of 0.8 m, the performance of the system has been explored at inlet temperature from 15 to 24°C with increments of 3°C. The system's averaged heat transfer efficiency was found to decrease with the increase in inlet temperature. This research provides valuable insight into the data centre information technology equipment cooling, which is of great significance for energy saving and environmentally friendly operation of data centres.

Keywords: data centre; cooling; micro-channel; separated loop heat pipe; experiment

*Corresponding author: zwang@gdut.edu.cn

Received 7 February 2020; revised 31 March 2020; editorial decision 19 May 2020; accepted 19 May 2020

1. INTRODUCTION

Information technology (IT) is now playing a prominent role in changing human life, e.g. smart transportation and smart communication, which has resulted in increasing interest in more advanced and energy-efficient data centres and HVAC (Heating, Ventilating and Air Conditioning) systems. However, the existing data centres consume a huge amount of energy in China and worldwide [1, 2]. In 2016, the total energy consumed by data centres around the world amounted for 416.2 billion kWh majority of which (30–40%) was consumed by the cooling systems in data centres [3, 4]. Thus, reducing cooling energy consumption and

improving cooling efficiency in data centres to achieve the zero or near-zero carbon buildings have been investigated by various research and technical works.

In traditional data centres, the cooling is achieved by directly pumping outdoor air into the data centre (free cooling) to maintain the indoor environment under required conditions, e.g. temperature in the range of 18–23°C [5, 6]. The indoor environments cooled in this way have shown to be capable of preserving the IT devices operating in the superior condition. The 'free cooling' method could avoid the use of a refrigeration unit and improve the service life of the cooler [7]. Mahdi *et al.* [8] proposed a combined free cooling and waste heat recovery system which

International Journal of Low-Carbon Technologies 2021, 16, 98–113 © The Author(s) 2020. Published by Oxford University Press.

This is an Open Access article distributed under the terms of the Creative Commons Attribution Non-Commercial License (http://creativecommons.org/licenses/by-nc/4.0/), which permits non-commercial re-use, distribution, and reproduction in any medium, provided the original work is properly cited. For commercial re-use, please contact journals.permissions@oup.com

contained an air-side economizer and a water-side economizer to reduce the energy consumption of a data centre, which showed that the novel system had the annual natural gas and electricity saving potentials of 15,000 m³ and 250 MWh respectively, and 267 t of annual CO₂ emission reduction. Yang et al. [9] studied the design and operation mode of different air conditioning systems, including free cooling mode, combined cooling mode and power failure and supply continuous cooling mode. The advantage of free cooling mode in energy saving was clearly observed that the reduced annual cost can be achieved than the conventional refrigeration system, and it was found that such cooling method can be used around 49.1% of the year. However, the shortcomings were also explicit, e.g. the gaseous and particulate contamination to the IT devices due to direct air blow to the indoor environment could endanger the reliability of the IT devices [10], local hotspot creation due to the uneven and low thermal distribution across the IT rooms and overcooling due to lack of an appropriate airflow control system [11].

The liquid cooling method has been applied to the data centre to resolve the local hotspot and overcooling problems. The working fluid (liquid) flowing across the IT devices is capable of transferring high-density dissipated heat energy and improving the heat transfer efficiency, which is also called 'self-cooling method' [12, 13]. Wu et al. [14] developed and tested an immersed jet array impingement-cooling device with the minimum total thermal resistance of 0.05 K/W and volume flow rate of 35 m³/s achieving the maximum effective heat transfer coefficient and found that the proposed system had better performance than the traditional cooling methods. Li et al. [15] proposed a cooling method using liquid-cooled servers to replace the selected air-cooled servers in data centres, which could effectively achieve up to 26.7% power consumption saving, which could help a data centre gain a full return on the capital investment in <3 years. However, liquid leakage can be a possible issue to the safe operation and security of data centres [13]. In addition, the noise and increased thermal resistance from the pump are other problems associated with the liquid cooling method.

With higher reliability and cooling efficiency demands in data centres, the heat pipe technology has been proposed by many studies. The heat pipe is an efficient heat transfer device transporting a large amount of heat from the evaporator to the condenser through a long distance within the desired operating temperature range, which can increase cooling efficiency by 3-5 times and decrease the PUE through integration with IT racks [5, 16, 17]. Sun et al. [18] tested a cooling system consisting of a separated heat pipe unit in which the cooling capacity reached nearly 200 kW, and the energy efficiency ratio changed from 21.2 to 3.1 under the outdoor temperature increasing from -5to 45°C. Wang et al. [19] studied the integrated cooling system combining the heat pipe cooling cycle and vapour compression cooling cycle. The thermodynamic analyses showed that the PUE of the data centre using this type of system could be 30% lower than the traditional air-cooling systems in cold areas. Tian et al. [20] proposed the new cooling system consisting of the internally cooled racks with two-stage heat pipe loops and combined water

loop with serially connected multi-cold sources, which effectively improved the reliability of data processing devices and reduced cooling energy cost by 46%. However, both the condenser and the evaporator of the heat pipe were positioned inside the data centre room, leading to the additional heat generation in the IT services that requires secondary cooling processes of the room air. Another issue was the installation of the heat pipe which was complicated due to modification of the IT racks, leading to a costly and time-consuming installation process.

In summary, air cooling, liquid cooling and heat pipe cooling have their own advantages and disadvantages, and the comparison of the three methods of cooling is shown in Table 1.

In this paper, a novel micro-channel flat separated loop heat pipe (MCSLHP) system has been proposed and investigated using numerical and experimental analyses. The proposed system consists of indoor and outdoor modules. The indoor module could be pre-fabricated and directly attached to the inside panels of the IT racks, while the outdoor module is placed outside the data centre, receiving the heat discharged from the IT devices and reducing the cooling load in the data centre for further use. The performance of the system was numerically studied under different inlet water temperatures. Under the specified condition, the tests were conducted, and the test results were used to validate the numerical model. This study provides a novel and efficient solution for data centre cooling, which is low-cost, has easy installation and is very effective in achieving zero or near-zero carbon data centre.

2. SYSTEM DESCRIPTION

Based on the analysis of various types of heat pipe cooling systems, which was studied by other researchers and to overcome the above addressed difficulties, a novel micro-channel flat separated loop heat pipe system was designed. The proposed system, as shown in Figure 1, consists of three parts: (1) indoor module which is the micro-channel heat pipe evaporator of MCSLHP placed in the IT rack; (2) outdoor module which is the microchannel heat exchanger including the micro-channel heat pipe condenser of MCSLHP, the water tank and the water pump as shown in Figure 2; and (3) vapour/liquid refrigerant pipe. In order to improve the heat transfer performance, the system could be charged with different refrigerants like R134a or R410a [21]. It should be mentioned that the optimal filling ratio was different with different refrigerants, and the compatibility of the refrigerant with the heat pipe wall should also be considered.

The working principle of the system is illustrated as follows. In the indoor module, the micro-channel heat pipe evaporator is placed directly under the bottom surface of the IT equipment and closely attached by using the thermal grease. When the evaporator receives heat from the IT equipment, the heat will be absorbed by the refrigerant inside, and the remaining is dissipated into the surroundings due to the temperature difference between the evaporator surface and ambient. As a result, the refrigerant within the micro-channel evaporator is converted into vapour, and this vapour gathers at the vapour refrigerant pipe by the buoyancy

Table 1. Comparison of three methods of cooling.

Cooling methods	Advantages	Disadvantages
Air cooling	Low initial cost, short payback period, energy saving and environmental protection.	Particle pollution, uneven cooling distribution, possible influence to the reliability of the IT devices.
Liquid cooling	Decreasing the occurrence possibility of local hotspot and problem of overcooling, being capable of quickly transmitting high-density heat radiation and improving heat transfer efficiency comparing with air cooling.	Possible liquid leakage, and high noise and thermal resistance due to the pump.
Heat pipe cooling	Long-distance and effective heat transfer, high heat transfer efficiency.	High installation cost.

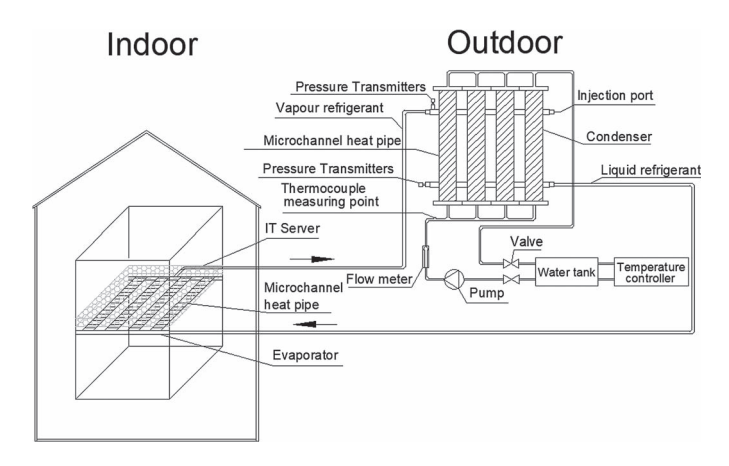


Figure 1. The schematic of the MCSLHP cooling system.

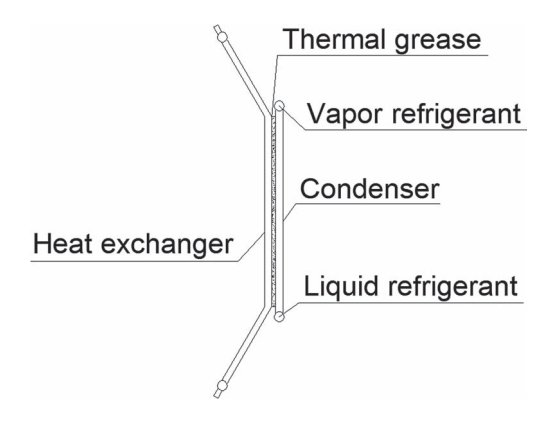


Figure 2. The connection of the micro-channel heat exchanger.

effect. In the vapour pipe, the vapour flows to the condenser (outdoor module) due to the high-temperature vapour pressure. Within the condenser, the vapour in the interior channel transfers heat to the water by the heat exchanger, leading to the gradual condensation of the vapour. The condensed liquid will fall into the liquid refrigerant pipe where the vapour is completely condensed at the end of the channels. In the liquid pipe, the refrigerant liquid will flow to the evaporator (indoor module) by gravity and capillary force. At the same time, the tank water is heated and driven by pump to the building for hot water supply.

The characteristics of the proposed novel cooling system could be summarized in the following five aspects.

- (1) The specialized MCSLHP combined a number of innovations, e.g. micro-channel structure, flat structure and separated loop structure, leading to increased vapour pressure and improved heat absorption area.
- (2) The micro-channel flat heat exchanger is closely adhered to the condenser, which can have sufficient contact area enabling full condensation of the refrigerant.
- (3) Using refrigerant as the working fluid can avoid the highpressure operation of the heat pipe and minimize the risk of leakage.
- (4) The indoor and outdoor module ensures the remote operation of transferring heat generated from data centre IT equipment, leading to reduced data centre air conditioning energy consumption and potentially improve the heat utilisation of the waste heat.
- (5) The novel system provides a simple and flexible structure of the separated cooling system, which means that the two modules can be positioned according to the actual situation on site. For the data centres employing traditional cooling systems, the system can be re-fabricated without changing the original pattern of the data centre and occupying additional space for the new system.

3. MATHEMATICAL ANALYSIS AND COMPUTER-MODELLING SET-UP

3.1. Determining the heat transfer capacity of the MCSLHP

The heat transfer capacity of the MCSLHP should be determined as it governs the maximum amount of heat transferring. Since the MCSLHP is a particular type of loop heat pipe, the heat transfer capacity is the least of the capillary, entrainment, viscous, boiling, sonic and filled liquid mass limits.

$$Q_{\min} = (Q_{\text{CL}}, Q_{\text{EL}}, Q_{\text{BL}}, Q_{\text{SL}}, Q_{\text{FL}})_{\min}$$
 (1)

The capillary limit indicates the capability of the micro-channel groove to carry liquid flow for heat transfer. During the operation, the sum of the capillary force and gravity will be higher than or equal to the total amount of flow resistances from the liquid and

vapour [22].

$$Q_{\rm CL} = \frac{K\sigma_l \rho_l h_{fg} A_w}{\mu_l L_{ef}} \cdot \left(\frac{2}{r_{ef}} - \frac{\rho_l g L_{hp} \cos \theta}{\sigma_l}\right) \tag{2}$$

Entrainment limits happen only in the evaporator and condenser caused by vapour flow entraining with the liquid, which will reduce the amount of liquid evaporation and eventually result in the 'dry-out' problem [23]. Therefore, the smaller value of the entrainment limits in the evaporator and condenser will be the entrainment limit of the system.

$$Q_{\rm EL} = \left(Q_{\rm EL,e}, Q_{\rm EL,c}\right)_{\rm min} = \frac{\pi}{4} z h_{fg} (\sigma_{\nu} \rho_{\nu})^{0.5} \cdot \begin{bmatrix} \frac{N_{e} (D_{e} - 2\delta_{e})^{2}}{D_{w,e}^{0.5}}, \\ \frac{N_{c} (D_{c} - 2\delta_{c})^{2}}{D_{w,c}^{0.5}} \end{bmatrix}_{\rm min}$$
(3)

Viscous limits happen mainly in the vapour phase flow, i.e. evaporator, vapour pipe and condenser. High vapour viscosity leads to reduced amount of heat carried by the vapour flow [24]. Therefore, the smallest value of the viscous limits in the evaporator, vapour pipe and condenser will be the viscous limit of the system.

$$Q_{VL} = (Q_{VL,e}, Q_{VL,\nu l}, Q_{VL,c})_{min}$$

$$= \frac{\pi z h_{fg} P_{\nu} \rho_{\nu}}{256 \mu_{\nu}} \cdot \begin{bmatrix} \frac{N_{e} (D_{e} - 2\delta_{e})^{4}}{L_{e}}, \\ \frac{N_{\nu l} (D_{\nu l} - 2\delta_{\nu l})^{4}}{L_{\nu l}}, \\ \frac{N_{e} (D_{e} - 2\delta_{e})^{4}}{L_{e}}, \end{bmatrix}_{min}$$
(4)

Boiling limits happen in the evaporator and condenser caused the high operational temperature of the refrigerant. In this case, the refrigerant may evaporate leading to a 'dry-out' problem, and then the heat pipe stops working [24, 25]. It should be mentioned that $P_{c,\max}$ in Eq. (5) is the maximum capillary power, which can be ignored by comparing with the value of $2\sigma_v/r_b$ [26]. Therefore, the smaller value of the boiling limits in the evaporator and condenser will be the boiling limit of the system.

$$Q_{\text{BL}} = \left(Q_{\text{BL},e}, Q_{\text{BL},c}\right)_{\text{min}}$$

$$= \begin{cases} \left[\frac{2\pi T_c \lambda_w L_e N_e z}{h_{fg} \rho_v \ln(D_e/(D_e - 2\delta_e))} \cdot \left(\frac{2\sigma_v}{r_b} - P_{c,\text{max}}\right)\right], \\ \left[\frac{2\pi T_c \lambda_w L_c N_c z}{h_{fg} \rho_v \ln(D_c/(D_c - 2\delta_c))} \cdot \left(\frac{2\sigma_v}{r_b} - P_{c,\text{max}}\right)\right] \end{cases}_{\text{min}}$$

$$= \frac{4\pi z \sigma_v \lambda_w}{h_{fg} \rho_v r_b} \cdot \left[\frac{\frac{T_e L_e N_e}{\ln(D_e/(D_e - 2\delta_e))}, \\ \frac{T_c L_c N_c}{\ln(D_c/(D_c - 2\delta_c))} \right]_{\text{min}}$$
(5)

Sonic limits happen in the evaporator, vapour pipe and condenser where the vapour velocity is close to the sonic or supersonic level due to the high-temperature operation of the refrigerant. Then, the operation will accompany with noise, and even worse, the heat pipe is blocked leading to vibration and breakdown [24]. Therefore, the smallest value of the sonic limits

in the evaporator, vapour pipe and condenser will be the sonic limit of the system.

$$Q_{SL} = (Q_{SL,e}, Q_{SL,vl}, Q_{SL,c})_{\min}$$

$$= \frac{\pi z \rho_v h_{fg} C_v^{0.5} \gamma^{0.5}}{4\sqrt{2}(\gamma+1)^{0.5}} \cdot \begin{bmatrix} T_e^{0.5} N_e (D_e - 2\delta_e)^2, \\ T_{vl}^{0.5} N_{vl} (D_{vl} - 2\delta_{vl})^2, \\ T_c^{0.5} N_c (D_c - 2\delta_c)^2 \end{bmatrix}_{\min}$$
(6)

Filled liquid mass limits happen in the liquid refrigerant pipe and condenser which describe the limitation of the refrigerant mass charged into the system owing to the influence of gravity [24]. Therefore, the smaller value of the filled liquid mass limits in the liquid refrigerant pipe and condenser will be the filled liquid mass limit of the system.

$$Q_{\text{FL}} = (Q_{\text{FL,ll}}, Q_{\text{FL,c}})_{\min} = \frac{g h_{fg}}{3x^3 \pi^2 \mu_l \rho_l} \cdot \begin{pmatrix} \frac{m_{ll}^3}{D_{ll}^2 N_{il}^2 L_{ll}^3}, \\ \frac{m_c^3}{D_{w,c}^2 N_c^2 L_{w,c}^3} \end{pmatrix}_{\min}$$
(7)

3.2. Analysing the heat transfer processes of the MCSLHP

Heat transfer occurring in the MCSLHP involves three processes, i.e. heat absorption by the evaporator Q_e , heat transfer from the evaporator to the condenser via evaporation and condensation of the refrigerant Q_{e-c} and heat output from the condenser Q_c . These processes are interrelated and dependent, until a balanced condition is achieved [24]. To simplify the heat transfer analysis, the temperatures of the evaporator surface (T_e) and condenser surface (T_c) are assumed to be stable.

$$Q_e = Q_{e-c} = Q_c \tag{8}$$

It must be noted that the steady-state heat transfer from the evaporator to the condenser via evaporation and condensation of the refrigerant Q_{e-c} should compare with the heat transfer capacity of the MCSLHP Q_{\min} as in Eq. (9) and Eq. (10). If Q_{e-c} is less than or equal to Q_{\min} , it means that the MCSLHP has the ability to transfer sufficient amount of heat that the MCSLHP can work properly, while if Q_{e-c} is larger than Q_{\min} , a large amount of heat would be accumulated since the system should work under the limitation of the heat transfer capacity, leading to the dryout problem of the heat pipe, and finally the MCSLHP will stop working.

If
$$Q_{e-c} \le Q_{\min}$$
, the MCSLHP works properly. (9)

If
$$Q_{e-c} > Q_{min}$$
, the MCSLHP stops working. (10)

The heat absorbed by the evaporator of the MCSLHP (Q_e) equals to the heat absorbed at the IT equipment (Q_i) minus the

heat losses from the surface of the evaporator to the ambient $(Q_{loss,e})$ [27, 28].

$$Q_{e} = Q_{i} - Q_{\text{loss},e} = \alpha P_{\text{IT}} - \frac{A_{e} N_{e} \sigma_{e} \varepsilon_{e} h_{\text{amb}} \left(T_{e}^{4} - T_{\text{amb}}^{4}\right)}{\sigma_{e} \varepsilon_{e} \left(T_{e} + T_{\text{amb}}\right) \left(T_{e}^{2} + T_{\text{amb}}^{2}\right) + h_{\text{amb}}}$$
(11)

The heat transferring from the evaporator to the condenser via evaporation and condensation of the refrigerant (Q_{e-c}) equals the heat absorbed by the evaporator of the MCSLHP (Q_e) [26]. In this process, several thermal resistances are involved to determine the effectiveness of the heat transfer in the MCSLHP, i.e. evaporator wall resistance (R_e) , groove resistance (R_w) and vapour flow resistance (R_{ν}) [27, 29, 30].

$$Q_{e-c} = \frac{T_e - T_v}{R_e + R_w + R_v}$$

$$= \frac{T_e - T_v}{\left\{\frac{1}{2\pi} \cdot \left[\left[\frac{\ln(D_{eo}/D_{ei})}{L_e \lambda_e N_e}\right] + \left[\frac{\ln(D_{ei}/(D_{ei} - 2\delta_e))}{L_w \lambda_w N_w}\right]\right] + \left\{\frac{T_v}{\rho_v^2 h_{fg}^2} \cdot \left[\frac{2m_v}{(D_{ei} - 2\delta_w)^4 N_e} + \frac{128\mu_v L_{vl}}{\pi D_{vl}^4} + \frac{8m_v}{\pi^2 (D_{ci} - 2\delta_{lf})^4 N_c}\right]\right\}}$$
(12)

The heat output from the condenser (Q_c) will be partially dispersed to the ambient due to the high condenser temperature $(Q_{loss,c})$, and the remaining will be transferred to water (Q_o) [27, 28].

$$Q_{o} = Q_{c} - Q_{\text{loss},c}$$

$$= \frac{T_{v} - T_{c}}{R_{lf} + R_{c}} - \frac{A_{c}N_{c}\sigma_{c}\varepsilon_{c}h_{\text{amb}}\left(T_{c}^{4} - T_{\text{amb}}^{4}\right)}{\sigma_{c}\varepsilon_{c}\left(T_{c} + T_{\text{amb}}\right)\left(T_{c}^{2} + T_{\text{amb}}^{2}\right) + h_{\text{amb}}}$$

$$= \frac{2\pi\left(T_{v} - T_{c}\right) \cdot L_{lf}\lambda_{lf}N_{lf} \cdot L_{c}\lambda_{c}N_{c}}{\left[\ln\left(D_{ci}/\left(D_{ci} - 2\delta_{lf}\right)\right) \cdot L_{c}\lambda_{c}N_{c}\right] + \left[\ln\left(D_{co}/D_{ci}\right) \cdot L_{lf}\lambda_{lf}N_{lf}\right]}$$

$$- \frac{A_{c}N_{c}\sigma_{c}\varepsilon_{c}h_{\text{amb}}\left(T_{c}^{4} - T_{\text{amb}}^{4}\right)}{\sigma_{c}\varepsilon_{c}\left(T_{c} + T_{\text{amb}}\right)\left(T_{c}^{2} + T_{\text{amb}}^{2}\right) + h_{\text{amb}}}$$
(13)

3.3. Calculating the heat transfer efficiency of the **MCSLHP**

The heat transfer efficiency of the proposed MCSLHP system is calculated from the heat output transferred to the water (Q_0) divided by the heat absorbed at the IT equipment (Q_i) [31].

$$\eta = \frac{Q_o}{Q_i} \times 100\% \tag{14}$$

3.4. Computer modelling set-up

The algorithm used for the modelling set-up is presented in a flow chart as shown in Figure 3, which can be summarized as follows:

- 1) Input operating conditions, e.g. ambient temperature, heat source power, water flow rate and water inlet temperature; and structural parameters, e.g. height difference between evaporator and condenser of MCSLHP, width and length of each micro-channels and length and diameter of refrigerant
- 2) Input refrigerant parameters, e.g. working temperature, filling ratio.
- 3) Calculate the six heat transfer limits (Q_{VL} , Q_{SL} , Q_{EL} , Q_{CL} , $Q_{\rm BL}$, $Q_{\rm FL}$) using Eqs. (2)–(7) and determine the heat transfer capacity of the MCSLHP (Q_{min}) using Eq. (1).
- 4) Determine the heat generated from the IT equipment (Q_i) and heat losses from the surface of the evaporator to the ambient ($Q_{loss,e}$), and calculate the initial heat absorbed by the evaporator (Q_e) using Eq. (11).
- 5) Compare Q_e and Q_{min} using Eqs. (9) and (10). If $(Q_e Q_{\min}$)/ $Q_e > 0.001$, then return to step 1) for recalculation, while if $(Q_e - Q_{\min})/Q_e \le 0.001$, then determine the heat absorbed by the evaporator (Q_e) .
- 6) Compare Q_e and Q_{e-c} . If $(Q_e Q_{e-c})/Q_e > 0.001$, then return to Step 1 for recalculation; while if $(Q_e - Q_{e-c})/Q_e \le 0.001$, then determine the heat transferring from the evaporator to the condenser via evaporation and condensation of the refrigerant (Q_{e-c}) by Eq. (12).
- 7) Compare Q_{e-c} and Q_c . If $(Q_{e-c} Q_c)/Q_{e-c} > 0.001$, then return to Step 1 for recalculation, while if $(Q_{e-c} - Q_c)/Q_{e-c} \le$ 0.001, then the whole system reaches stable, and the heat output from the condenser (Q_c) could be determined by
- 8) Calculate the heat losses from the surface of the condenser to the ambient $(Q_{loss,c})$, and determine the heat output transferred to water (Q_o) using Eq. (13).
- 9) Calculate the thermal efficiency of the system using Eq. (14).
- 10) Stop program.

Since the vapour refrigerant will be completely liquefied in the condenser, the sub-program has been set up for determining the optimal length of the condenser of the MCSLHP.

- 1) Assuming initial values of length of the condenser L = 0, input outlet water temperature $T_{wa,out}$, vapour refrigerant temperature T_{ν} and dryness of the refrigerant at the inlet of the condenser X0 = 1.
- 2) Assuming the length of the condenser L = L + 0.01.
- 3) Assuming dryness of the refrigerant at the outlet of the condenser $XN = X0-10^{-8}$.
- Calculate the latent heat exotherm $Q_1 = r_{wa} m_{wa} (X0 XN)$. Assuming the heat transferred to water $Q_2 = Q_1 - Q_{loss,c}$, calculate the inlet water temperature $T_{\text{wa,in}} = T_{\text{wa,out}} 2[T_v - (R_c + R_w + R_{lf}) * Q_1]$ and the total heat absorbed by water $Q_3 = c_{\text{wa}} m_{\text{wa}} (T_{\text{wa,out}} - T_{\text{wa,in}})$. Compare Q_2 and Q_3 . If $(Q_2 - Q_3)/Q_2 \ge 0.001$, then assuming $X_0 = X_0$ and

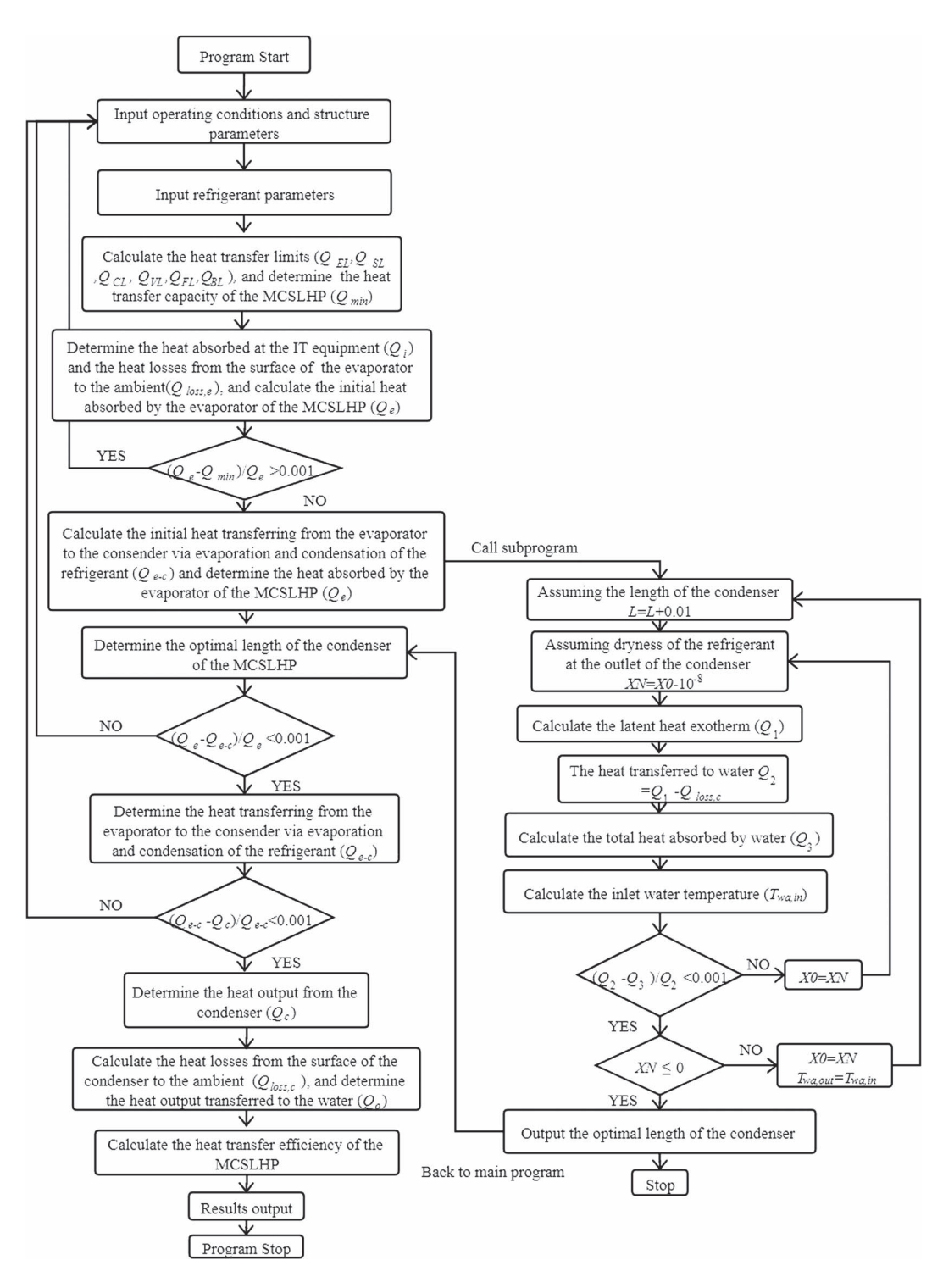


Figure 3. Flow chart for the modelling set-up.

- go to Step 2 of the sub-program for recalculation; while if $(Q_2 - Q_3)/Q_2 < 0.001$, then determine if $XN \le 0$.
- 5) If XN < 0, then return back to the main program and output the optimal length of the condenser; while if XN > 0, then assume X0 = XN and $T_{\text{wa,out}} = T_{\text{wa,in}}$, and return to Step 1 of the sub-program for recalculation.

4. TEST RIG CONSTRUCTION AND **EXPERIMENTAL ANALYSIS**

4.1. Test rig construction

Based on the system design from the established program and to validate the system's performance, a test rig was established at the laboratory of the Guangdong University of Technology, China.

The indoor module shown in Figure 4 was placed inside the data cabinet positioned in the Environmental Control Chamber, which consisted of the evaporator of MCSLHP including four micro-channels flat plates (as shown in Figure 5), vapour collecting pipe (25 mm in diameter and 484 mm in length) and liquid dividing pipe (20 mm in diameter and 500 mm in length). The size of the evaporator of the MCSLHP is 800 mm in length, 440 mm in width and 3 mm in thickness. Each micro-channel flat plate of the evaporator has 28 micro-channels with width and thickness of 3 mm, and each micro-channel contains 8 microgrooves with width and thickness of 0.7 mm. The outdoor module shown in Figure 6 was placed outside the Environmental Control Chamber, which included two parts, i.e. heat exchange part and water flow temperature control part. The heat exchange part shown in Figure 6a and b includes the condenser of the MCSLHP, heat exchanger, vapour dividing pipe (20 mm in diameter and 624 mm in length) and liquid collecting pipe (25 mm in diameter and 654 mm in length). The condenser of the MCSLHP and heat exchanger had similar structures as the evaporator, and the only difference was that the length of the condenser was 500 mm, and the length of the heat exchanger 900 mm. The heat exchanger was connected to the water tank through the water pump and water inlet/outlet pipe. The condenser and heat exchanger were closely attached using the thermal grease as shown in Figure 6b. As for the water flow temperature control part in Figure 6c, the inlet water temperature was controlled by the temperature controller (KL-003F model) to make sure the system is operating stably. All the pipes were insulated to minimize the heat losses to the ambient. The indoor and outdoor modules were then connected by the vapour refrigerant pipe (length and diameter of 1,800 mm and 20 mm, respectively) and liquid refrigerant pipe (length and diameter of 2,000 mm and 20 mm, respectively). The main parameters of the system components are shown in Table 2.

Since one CPU rack-mount server possesses the server heat load at 1,000-1,200 W [32], one heat source made of cast aluminium heating plate was used as the replacement of the IT equipment (e.g. server). A voltage regulator adjusted the simulated heat radiation, and an electric power detector was used to monitor the operating status of the heat source in real time. The vapour pres-

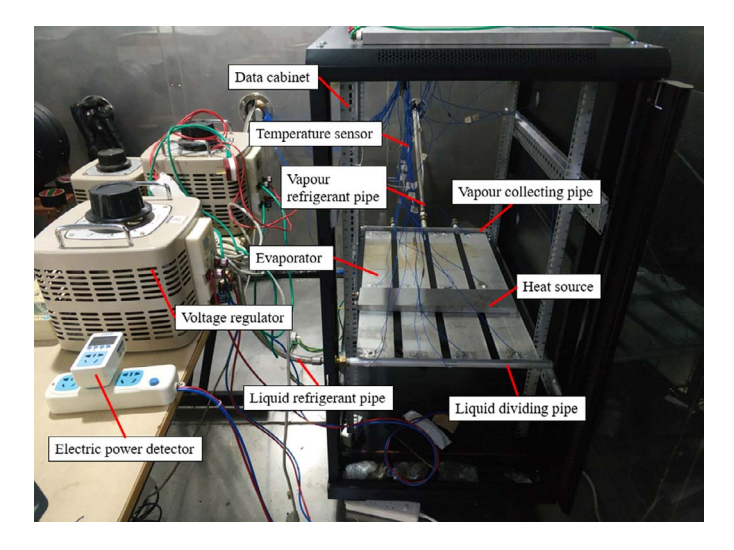


Figure 4. Schematic of the indoor module.

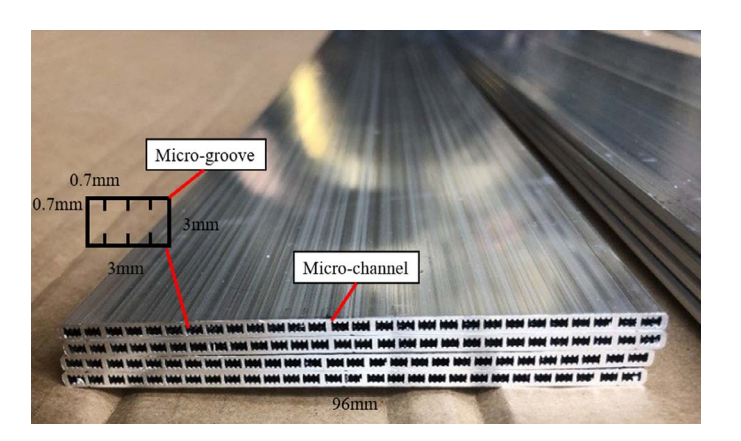


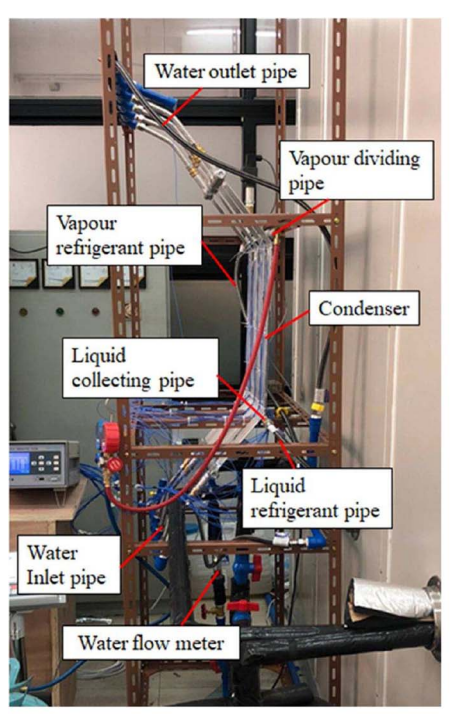
Figure 5. Inner structure of the micro-channel flat plate.

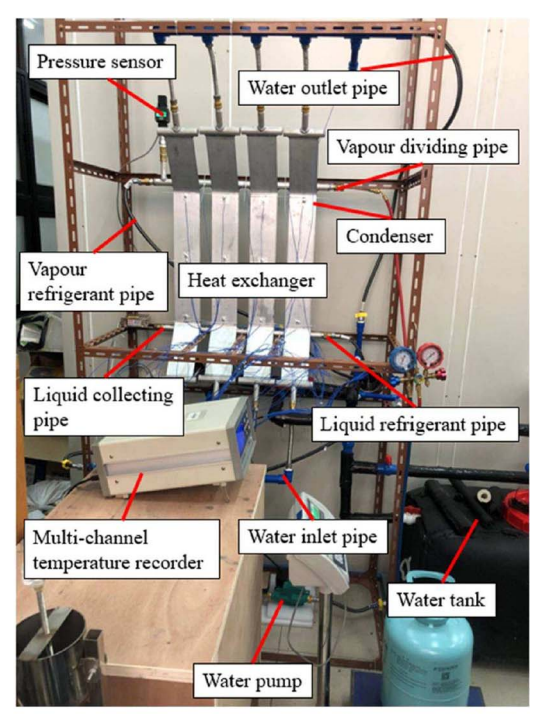
sure of the refrigerant in the MCSLHP was measured using the pressure sensor, and the flow rate and temperature of the water in the heat exchange part were measured using the water flow meter and temperature controller, respectively. The temperatures of the evaporator, the condenser of the MCSLHP and the heat exchanger were measured and recorded using the multi-channel temperature recorder (measuring points are shown in Figure 7). During the testing period of 1.5 h, the test data were recorded every 30 s. The main parameters of the test equipment are shown in Table 3.

4.2. Experimental steps

The experimental steps were as follows:

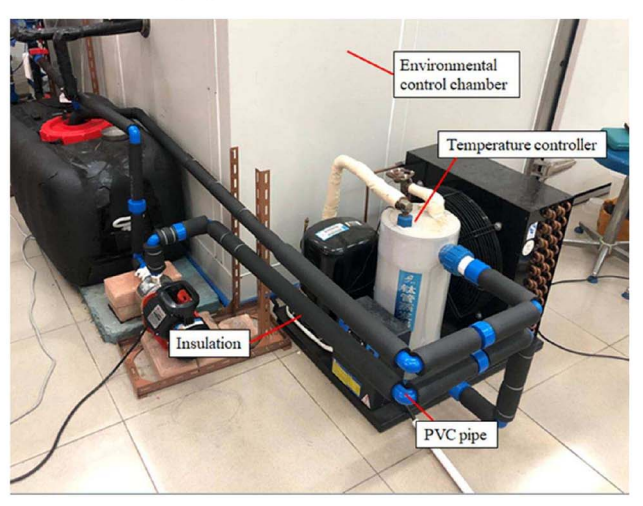
- 1) Set the ambient temperature of the environmental control chamber.
- 2) Vacuum the MCSLHP using the vacuum pump, and then charge the refrigerant (R134a with the filling ratio at 30%)
- 3) Turn on the temperature controller, water pump and water flow meter.





(a) front view of heat exchange part

(b) side view of heat exchange part



(c) water flow temperature control part

Figure 6. Schematic of the outdoor module: (a) front view of heat exchange part, (b) side view of heat exchange part, (c) water flow temperature control part.

Table 2. *Parameters of the system components.*

Components	Length (L) (mm)	Width (wi) (mm)	Thickness (δ) (mm)	Diameter (D) (mm)	Quantity (N)
Evaporator	800	440	3	_	1
Condenser	500	440	3	_	1
Heat exchanger	900	440	3	_	1
Vapour collecting pipe	484	_	_	25	1
Liquid dividing pipe	500	_	_	20	1
Liquid collecting pipe	654	_	_	25	1
Vapour dividing pipe	624	_	_	20	1
Vapour refrigerant pipe	1,800	_	2	20	1
Liquid refrigerant pipe	2,000	_	2	20	1

Table 3. *Parameters of the testing equipment.*

No.	Item	Model	Parameters
			Sensor: nickel chromium-nickel silicon (Type K);
	Multi-channel temperature recorder	JK-8/16 AT4532	Size of the sensor: 1 cm*1 cm;
1			Temperature test range: $-50-1,000^{\circ}$ C;
1			Measurement accuracy: $0-\pm0.5\%$;
			Power supply: 220 V \pm 10%, 50 Hz \pm 2%;
			Temperature signal input channel: 64.
)	Water flow meter	LFS100	Accuracy (at 25°C): $0-\pm$ (4%);
	water now meter		Test range: 100-1,000 L/h.
,	Pressure sensor	MIK-PX300	Test range: -0.1 —2.5 MPa.
			Power supply: 220 V;
	Voltage regulator	TDGC2-5000VA	Voltage output: 0-250 V;
			Maximum power: 5,000 W.
			Power supply: 220 V;
	Electric power detector	ZJXED	Maximum current: 10 A;
			Maximum power: 2,200 W.
8	Tomporature controller	KL-003F	Power supply: 220 V;
	Temperature controller		Maximum power: 2,250 W.
			Power supply: 220 V/50 Hz;
1	Water pump	BJZ037-B	Power: 370 W;
			Rated flow: 1.5 m ³ /h

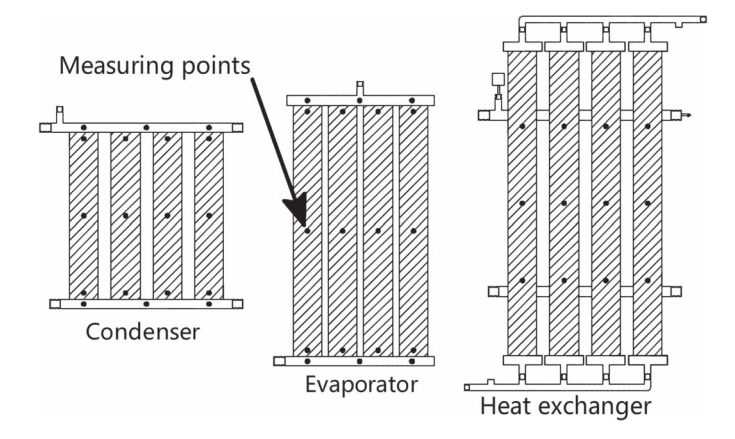


Figure 7. Temperature measuring points.

- 4) Install the temperature sensor to the system, and turn on the multi-channel temperature recorder.
- 5) Turn on and adjust the simulated heat source using the voltage regulator to the set value.
- 6) Observe the heat source power displayed on the electric power detector until it stabilizes.
- 7) The system starts to work.
- 8) Record the data shown in the multi-channel temperature recorder.
- 9) Turn off the system after operation period.
- 10) Process the recorded data.

RESULTS AND DISCUSSIONS

By varying the inlet water temperature from 15 to 24°C at every 3°C increment and keeping other parameter data unchanged (i.e.

simulated heat source at 1,000 W, water flow rate at 0.28 m³/h, ambient temperature at 26°C, refrigerant filling ratio at 30%, and the height difference between evaporator and condenser of the MCSLHP at 0.8 m), the temperature distribution and heat transfer efficiency of the MCSLHP system was investigated. Then, the results from the simulation and tests are compared under the same operating conditions for the system.

5.1. Temperature distribution

Figures 8–19 show the temperature variations of the heat exchanger, condenser and evaporator surfaces during the sable operating period. As to the heat exchanger, the temperature difference between the bottom and centre levels was higher than that between the top and centre levels (0.8–1.5°C) because the water entered from the bottom of the heat exchanger and absorbed the thermal energy directly from the condenser of the MCSLHP. The temperature of the heat exchanger surface increased with the increase in inlet water temperature. It was also found that when the inlet water temperatures were 15, 18, 21 and 24°C, the evaporator surface average temperatures were 23.1, 26.1, 29.5 and 31.0°C, and the condenser surface average temperatures were 23.7, 26.2, 29.5 and 31.0°C, respectively. The temperatures in the top, centre and bottom levels of the evaporator surface were in the difference range of <0.8°C, meaning that the heat generated from the heat source was evenly distributed on the surface of the evaporator. The temperature of the evaporator and condenser surfaces increased with the increase in inlet water temperature. This happened because of the condenser being closely attached to the heat exchanger, there is sufficient contact area for the refrigerant to completely condense (i.e. the calculated length of 420 mm is less than the experimental length of 500 mm for the condenser) and the

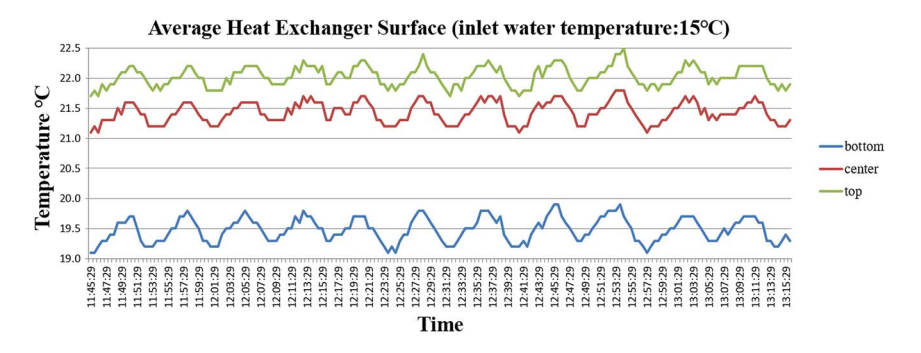


Figure 8. The variation of the average heat exchanger surface temperature with time for the system operated under the inlet water temperature of 15°C.

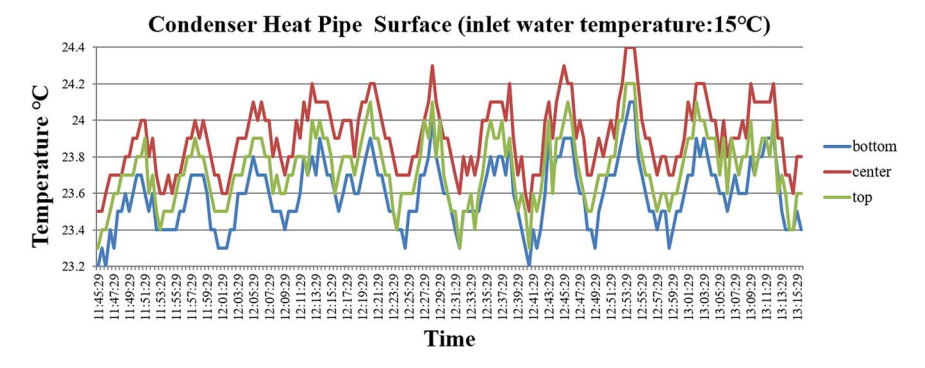


Figure 9. The variation of the average condenser surface temperature with time for the system operated under the inlet water temperature of 15°C.

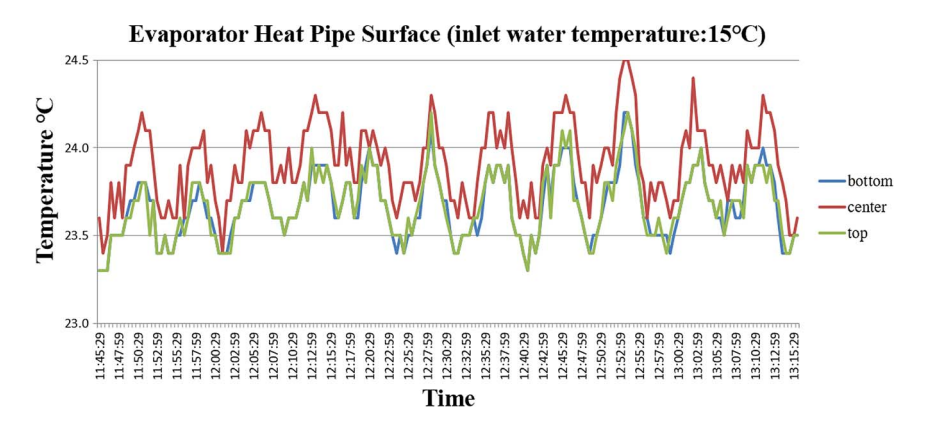


Figure 10. The variation of the average evaporator surface temperature with time for the system operated under the inlet water temperature of 15°C.

condenser surface temperature was directly influenced from the water flowing across the heat exchanger surface. In the meantime, since the MCSLHP operated under little pressure/temperature drop, the evaporator surface temperature will eventually rise up. It was also obvious that the temperatures of the heat exchanger, condenser and evaporator surfaces were fluctuating since the MCSLFP operated in the slow response from the evaporator to the condenser.

5.2. Heat transfer efficiency

Figures 20–23 present the variation of the instantaneous heat transfer efficiency with time during the operating period, and

Figure 24 summarizes the relationship of the average heat transfer efficiency with the inlet water temperature. The trend of the variation of the heat transfer efficiency with time was similar to that of the operating temperatures of the MCSLHP with time since it was affected by the operating temperature of the MCSLHP. When the inlet water temperature was at 15°C, the instantaneous heat transfer efficiency of the system ranged from 78.4 to 98%. From Figure 24, when the inlet water temperatures were 15, 18, 21 and 24°C, the average testing heat transfer efficiencies were 79.94, 77.46, 69.45 and 65.90%, respectively, and the average simulated heat transfer efficiencies were 82.56, 79.17, 75.78 and 72.39%, respectively. The linear relation of the average heat transfer efficiency with the inlet water temperature indicated that both

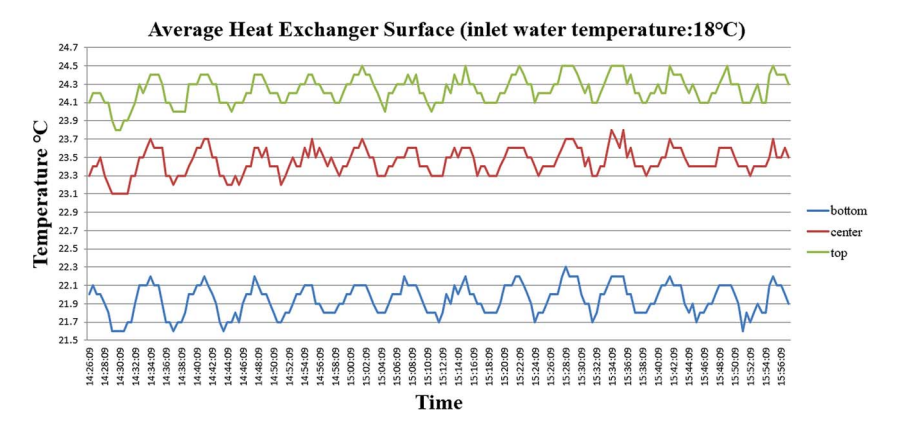


Figure 11. The variation of the average heat exchanger surface temperature with time for the system operated under the inlet water temperature of 18°C.

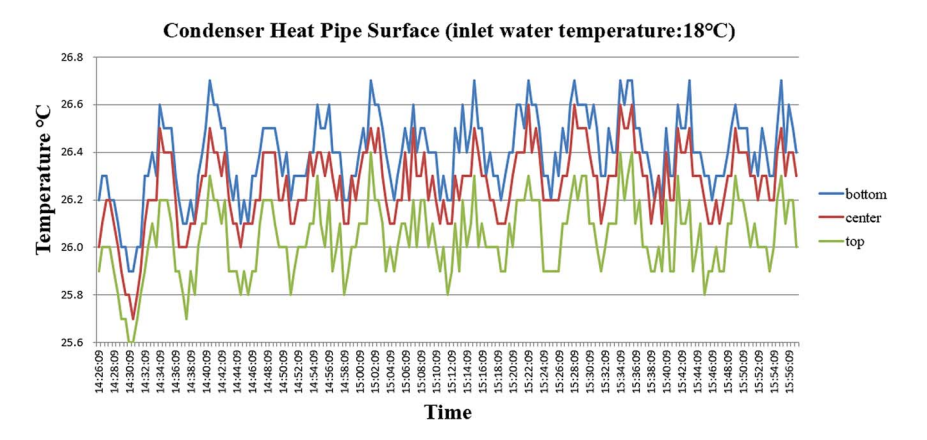
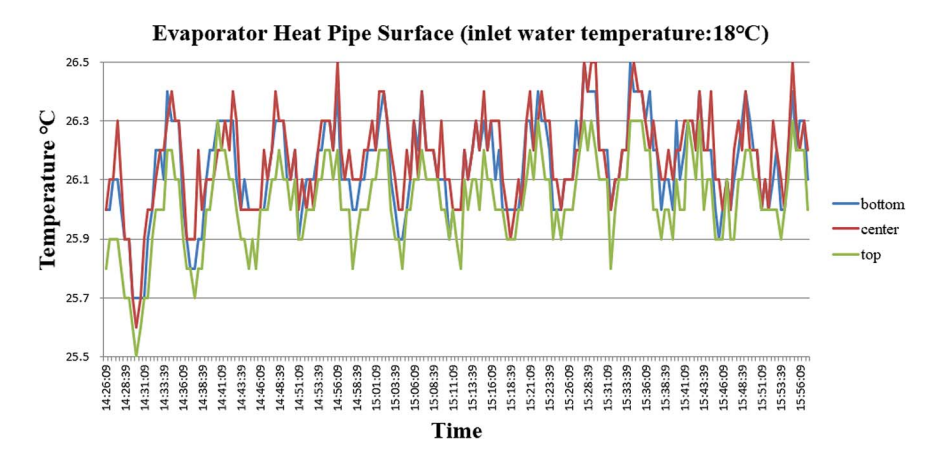


Figure 12. The variation of the average condenser surface temperature with time for the system operated under the inlet water temperature of 18° C.



 $\textbf{Figure 13.} \ \textit{The variation of the average evaporator surface temperature with time for the system operated under the inlet water temperature of 18°C.}$

average heat transfer efficiency from the tests and simulation results decreased with the increase in the inlet water temperature. When the inlet water temperature increased, the temperature difference between the water and refrigerant within the condenser decreased, leading to a reduced amount of heat transfer within the heat exchanger section and eventually the heat transfer efficiency.

5.3. Comparison of the simulation and testing results

From Figure 25, it was found that the error between the simulation and test results ranged from 2.16 to 8.97%, suggesting that the experiments and simulation results had a good agreement. It also indicated that the established model could predict the performance of the system with a good accuracy within the error range less than $\pm 10\%$, which can be used in practical

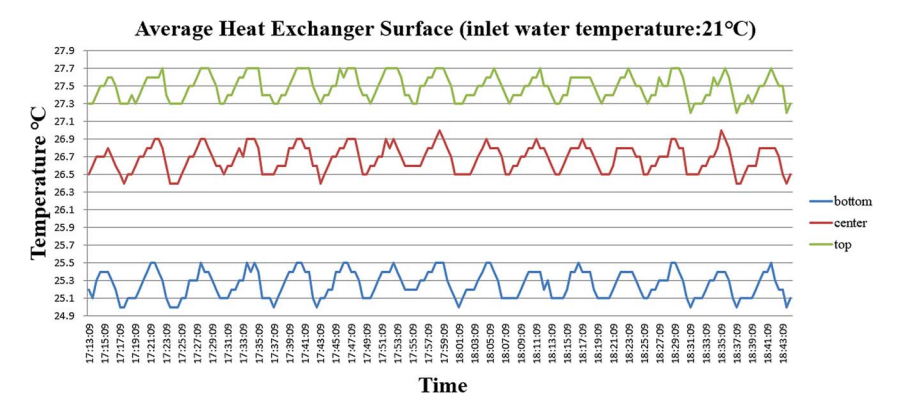


Figure 14. The variation of the average heat exchanger surface temperature with time for the system operated under the inlet water temperature of 21°C

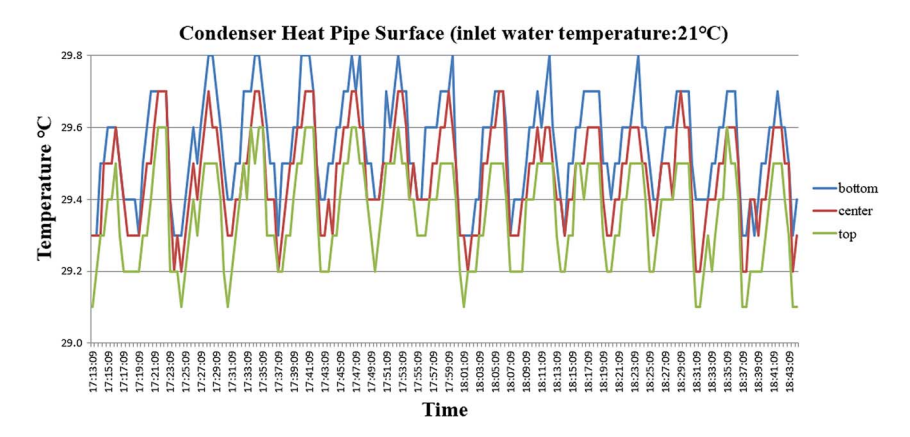


Figure 15. The variation of the average condenser surface temperature with time for the system operated under the inlet water temperature of 21°C.

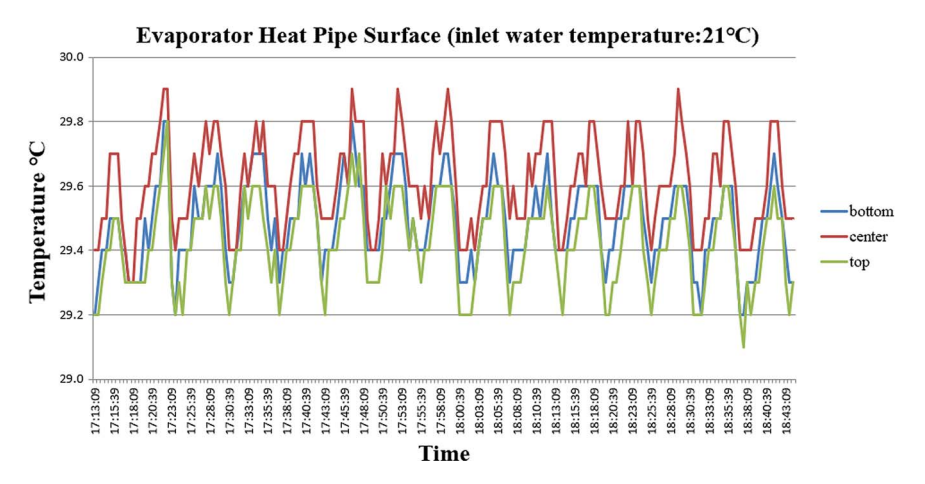


Figure 16. The variation of the average evaporator surface temperature with time for the system operated under the inlet water temperature of 21°C.

applications. The occurrence of the errors could have been caused from the experimental and simulation aspects. From the experimental aspect, it may be cause by heat losses occurring in the vapour/liquid refrigerant pipes during the tests due to the temperature difference between the pipes and the ambient, and the measurement error from the test equipment. From the simulation aspect, it may be cause by the simplified heat transfer calculation between the MCSLHP and surrounding air, missing the effect of the slow volume response of refrigerant in the MCSLHP.

5.4. Comparison of the proposed system with the conventional heat pipe cooling system

Zhou et al. [33] designed a heat pipe cooling system for data centre as shown in Figure 26. The evaporator and the condenser of the

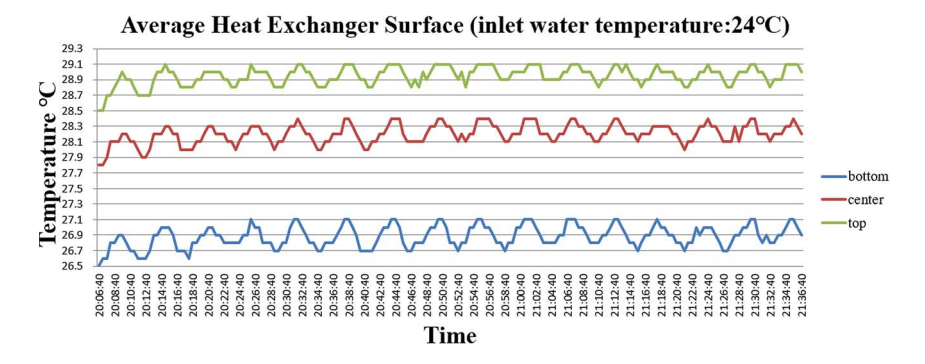


Figure 17. The variation of the average heat exchanger surface temperature with time for the system operated under the inlet water temperature of 24°C.

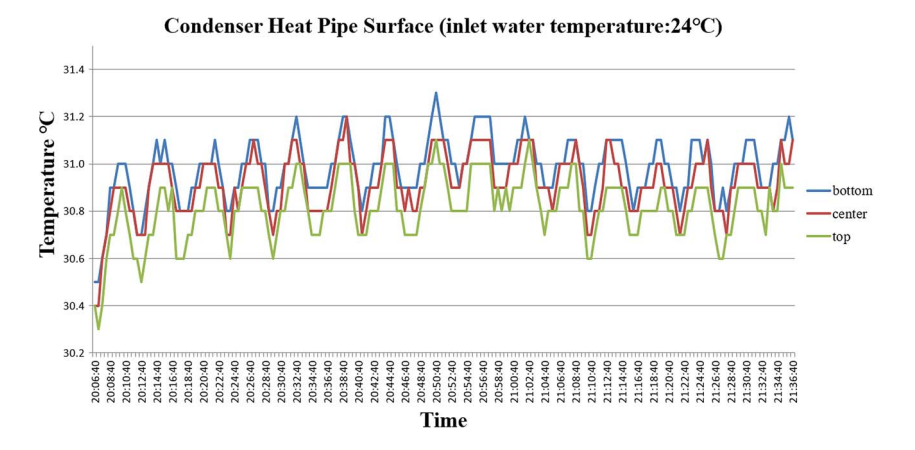


Figure 18. The variation of the average condenser surface temperature with time for the system operated under the inlet water temperature of 24°C.

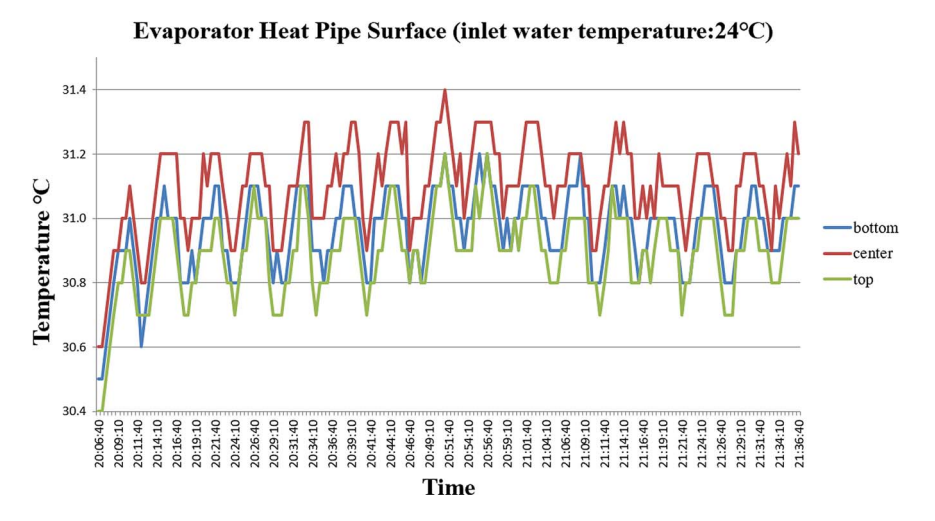


Figure 19. The variation of the average evaporator surface temperature with time for the system operated under the inlet water temperature of 24°C.

system developed by Zhou *et al.* [33] were made of ordinary heat pipes, and the evaporator was placed indoor next to the wall of the data centre, while the condenser was placed outdoor. Compared with the proposed system using the micro-channel flat loop heat pipe as the evaporator and the condenser, the energy consumption of the conventional heat pipe cooling system developed by Zhou *et al.* [33] was found at 2.20 kWh, while the energy consumption

of the proposed system was calculated at 0.56 kWh by using Eq. (15) [28] when both systems operated under the ambient temperature of 26°C and operating period of 1.5 h. As to the system COP, the conventional heat pipe system developed by Zhou *et al.* [33] reached 1.54, while the proposed system was at 2.7. There was a 74.77% increase in the COP of the proposed system. This increase can be explained from two aspects. First,

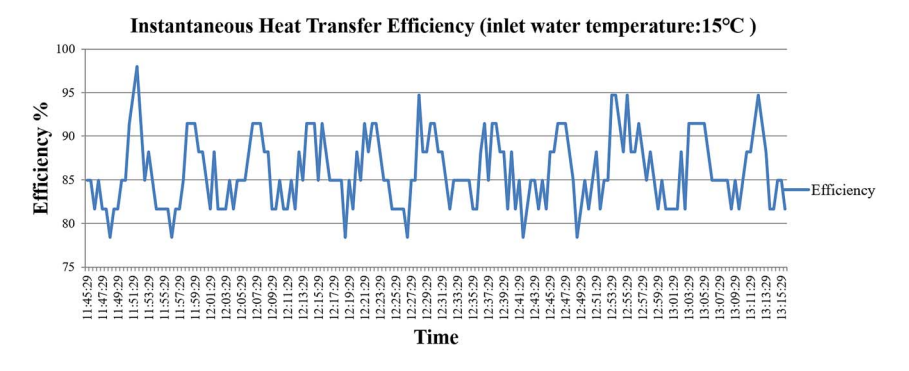


Figure 20. The variation of the instantaneous heat transfer efficiency with time for the system operated under the inlet water temperature of 15°C.

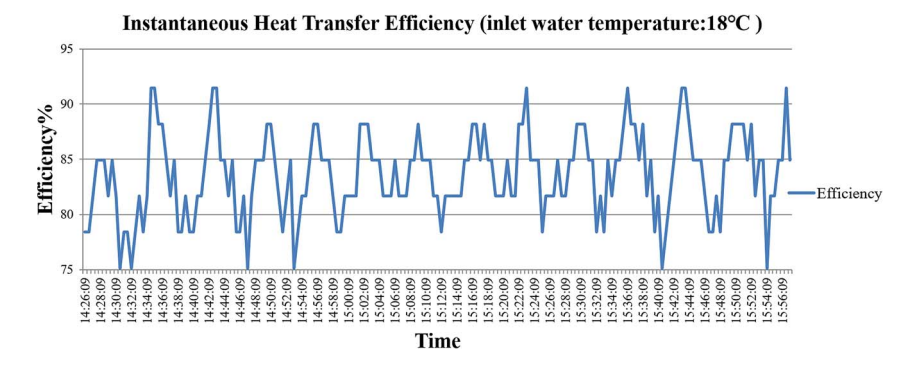


Figure 21. The variation of the instantaneous heat transfer efficiency with time for the system operated under the inlet water temperature of 18°C.

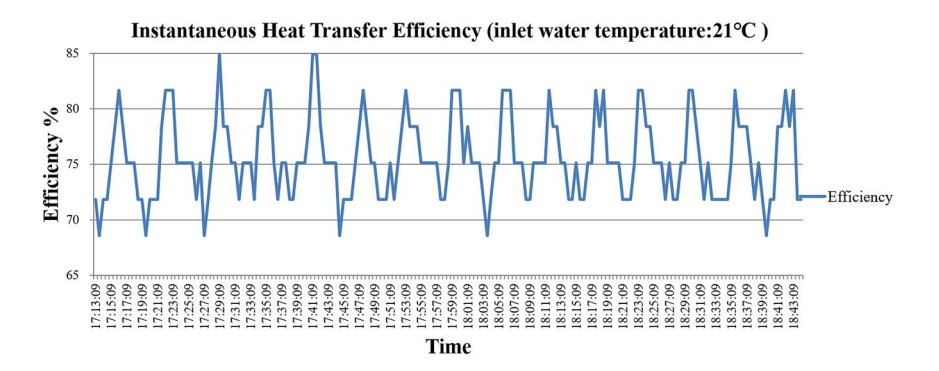


Figure 22. The variation of the instantaneous heat transfer efficiency with time for the system operated under the inlet water temperature of 21°C.

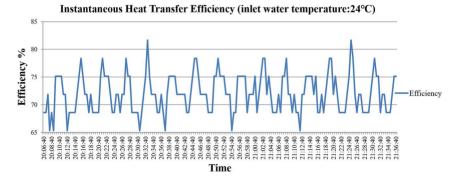


Figure 23. The variation of the instantaneous heat transfer efficiency with time for the system operated under the inlet water temperature of 24°C.

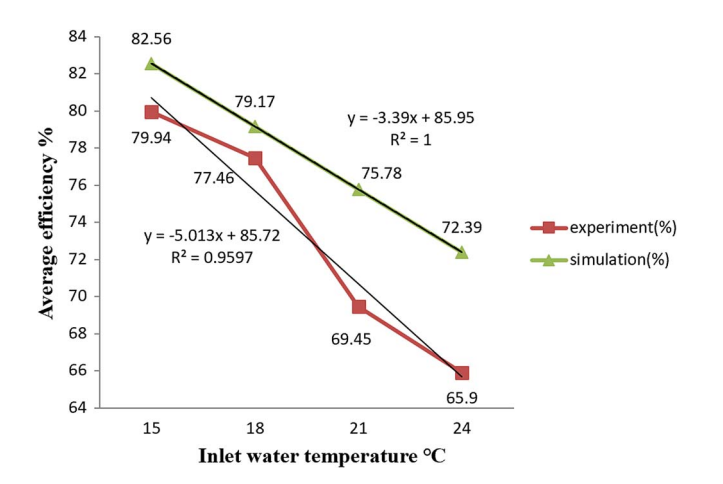


Figure 24. The average heat transfer efficiency against the inlet water temperature

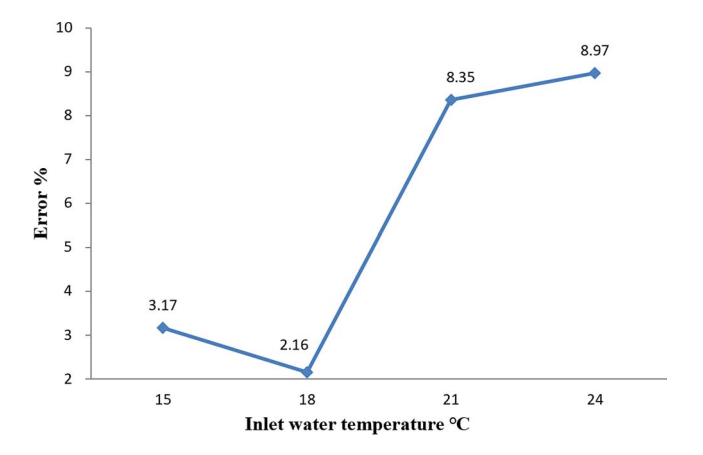


Figure 25. The error between the experimental and simulation results.

the micro-channel flat loop heat pipe of the proposed system contained micro-channels that increased the capillary pressure, and the condenser was placed vertically in the outdoor module that increased the gravity pressure, leading to increased driving force of the MCFLHP and eventually the increased vapour pressure. Second, the design of the flat evaporator was based on the IT equipment of the proposed system, which increased the heat absorption area comparing with the round shape of the conventional heat pipe.

$$W = P_{\text{pump}} \times t \tag{15}$$

6. CONCLUSIONS

This paper presented the experimental and numerical investigations of a novel micro-channel flat separated loop heat pipe (MCSLHP) system for cooling in the data centres. It was concluded that under the same operating conditions, the optimal

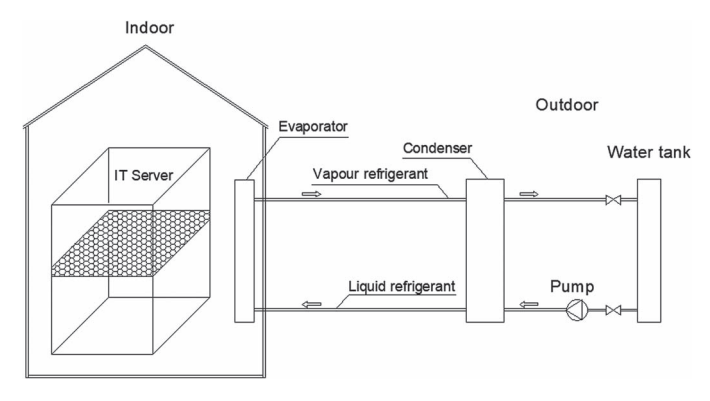


Figure 26. Schematic of the heat pipe cooling system investigated by Zhou et al.

water inlet temperature was 15°C leading to the maximum average heat transfer efficiency of 79.94%. The average heat transfer efficiency decreased with the increase in inlet water temperature. The comparison between the test and simulation results meant that the experiment and simulation results had a good agreement and that the established model can predict the performance of the system with good accuracy. In this case, the proposed MCSLHP system can be potentially used to remove the heat generated from the IT equipment in the rack, reduce the cooling load in the data centre room and realize the energy savings in data centre.

ACKNOWLEDGEMENTS

This work was financially supported by the National Key R&D Program of China (2016YFE0133300), Department of Science and Technology of Guangdong Province, China (2019A050509008), European Commission H2020-MSCA-RISE-2016 Programme (734340-DEW-COOL-4-CDC) and European Commission H2020-MSCA-IF-2018 Programme (835778-LHP-C-H-PLATE-4-DC).

REFERENCES

- [1] Onur K, Aslı GÖ. Comparison of sustainable information technologies for companies. Int J Low-Carbon Tech 2015;4:374-8.
- [2] Renewable Energy Unit. The European code of conduct on data centre energy efficiency. Version 3.0. European Commission 2015. https://e3 p.irc.ec.europa.eu/sites/default/files/files/documents/CoC documents/ introductory_guide_v3.0.0.pdf.
- [3] Zakarya M. Energy, performance and cost efficient datacenters: A survey. Renew Sust Energ Rev 2018;**94**:363–85.
- [4] Zhan B, Shao S, Zhang H, Tian C. Simulation on vertical microchannel evaporator for rack-backdoor cooling of data center. Appl Therm Eng 2020;164:114550. doi: 10.1016/j.applthermaleng.2019.114550.
- [5] Ni JC, Bai XL. A review of air conditioning energy performance in data centers. Renew Sust Energ Rev 2017;67:625-40.
- Sang H, Jun P, Jae J. Optimum supply air temperature ranges of various air-side economizers in a modular data center. Appl Therm Eng 2015;77:163-79.

- [7] Yong Y, Bo W, Zhou Q. Energy saving analysis of free cooling system in the data center. Procedia Eng 2017;205:1815-9.
- [8] Mahdi DD, Sajjad VN, Ahmad A. Simultaneous use of air-side and waterside economizers with the air source heat pump in a data center for cooling and heating production. Appl Therm Eng 2019;161:114133. doi: 10.1016/j.applthermaleng.2019.114133.
- [9] Yang Y, Wang B, Zhou Q. Air conditioning system design using free cooling technology and running mode of a data center in Jinan. Procedia Eng 2017;205:3545-9.
- [10] Kim J, Chang H, Jung Y et al. Energy conservation effects of a multistage outdoor air enabled cooling system in a data center. Energy Build 2017:138:257-70.
- [11] Ali H, Saman K. A review on efficient thermal management of air- and liquid-cooled data centers: From chip to the cooling system. Appl Energy 2017;205:1165-88.
- [12] Alfonso C, Giulio P. Cooling systems in data centers: State of art and emerging technologies. Energy Procedia 2015;83:484-93.
- [13] Ding T, He T, Hao T, Li Z. Application of separated heat pipe system in data center cooling. Appl Therm Eng 2016;109:207-16.
- [14] Wu R, Fan Y, Hong T et al. An immersed jet array impingement cooling device with distributed returns for direct body liquid cooling of high power electronics. Appl Therm Eng 2019;162:114259. doi: 10.1016/j.applthermaleng.2019.114259.
- [15] Li L, Zheng W, Wang X, Wang X. Data center power minimization with placement optimization of liquid-cooled servers and free air cooling. Sustain Comput-Inf Syst 2016;11:3-15.
- [16] Tian H. 2012. Research on cooling technology for high heat density data center. In Thesis for Doctor of Philosophy in Civil Engineering. Beijing, China: Tsinghua University.
- [17] Ong KS. Review of solar, heat pipe and thermoelectric hybrid systems for power generation and heating. Int J Low-Carbon Tech 2016;15:460-5.
- [18] Sun Y, Wang T, Yang L et al. Research of an integrated cooling system consisted of compression refrigeration and pump-driven heat pipe for data centers. Energy Build 2019;187:16-23.
- [19] Wang Z, Zhang X, Li Z, Luo M. Analysis on energy efficiency of an integrated heat pipe system in data centers. Appl Therm Eng 2015;90:937-44.

- [20] Tian H, He Z, Li Z. A combined cooling solution for high heat density data centers using multi-stage heat pipe loops. Energy Build 2015;94:177-88.
- Peterson GP. 1994. An Introduction to Heat Pipes: Modelling, Testing, and Applications. New York: Wiley-Interscience Press.
- Nemec P, Caja A, Malcho M. Mathematical model for heat transfer limitations of heat pipe. Math Comput Modell 2013;57:126-36.
- [23] Wang Z, Yang W. A review on loop pipe for use in solar water heating. Energy Build 2014;79:143-54.
- [24] Riffat SB, Zhao X, Doherty PS, Analytical and numerical simulation of the thermal performance of 'mini' gravitational and 'micro' gravitational heat pipes. Appl Therm Eng 2002;22:1047-68.
- [25] Bai L, Lin G, Mu Z, Wen D. Theoretical analysis of steady-state performance of a loop heat pipe with a novel evaporator. Appl Therm Eng 2014;64:
- [26] Chi SW. 1976. Heat Pipe Theory and Practice: A Sourcebook. US: McGraw-Hill Inc.
- [27] US Department of Energy. DOE fundamentals handbook: Thermodynamics, heat transfer and fluid flow, Volume 2 of 3, DOE-HDBK-1012/2-92. Washington DC, US: US Department of Energy, 1992.
- [28] Huang Q, Shao S, Zhang H, Tian C. Development and composition of a data center heat recovery system and evaluation of annual operation performance. Energy 2019;189:116200. doi: 10.1016/j.energy.2019.116200.
- Riffat SB, Zhao X, Doherty PS. Developing a theoretical model to investigate thermal performance of a thin membrane heat-pipe solar collector. Appl Therm Eng 2005;25:899-915.
- [30] Zhao X, Zhao X, Shen J et al. Dynamic performance of a novel solar photovoltaic/loop-heat-pipe heat pump system. Appl Energy 2014;114:
- [31] Qiu Z, Zhao X, Li P et al. Theoretical investigation of the energy performance of a novel MPCM (microencapsulated phase change material) slurry based PV/T module. Energy 2015;87:686-98.
- [32] Ali C, Dominic G. Cooling of server electronics: A design review of existing technology. Appl Therm Eng 2016;105:622-38.
- [33] Zhou F, Li C, Zhu W et al. Energy-saving analysis of a case data center with a pump-driven loop heat pipe system in different climate regions in China. Energy Build 2018;169:295-304.